PERGAMON

Vision Research 42 (2002) 1137–1148

Vision Research

www.elsevier.com/locate/visres

Isolation of stimulus characteristics contributing to Weber's law for position

David Whitaker [a,*], Arthur Bradley [b], Brendan T. Barrett [a], Paul V. McGraw [a]

[a] *Department of Optometry, University of Bradford, Bradford BD7 1DP, UK*
[b] *School of Optometry, 800 East Atwater, Indiana University, Bloomington, IN 47405, USA*

Received 29 January 2001; received in revised form 18 January 2002

Abstract

To examine the independent contribution of various stimulus characteristics to positional judgements, we measured vernier alignment performance for three types of Gabor stimuli. In one, only the contrast envelope of the upper and lower stimulus elements was offset, with the luminance-modulated carrier grating remaining in alignment. In the second, only the carrier grating was offset. In the third, both carrier and envelope were offset together. Performance was examined over a range of element separations. When both cues are available, thresholds for small separations are dominated by carrier offset information and are inversely proportional to carrier frequency. At large separations, thresholds are governed by the spatial scale characteristics of the envelope. For broadband stimuli such as lines, bars or dots typically used for vernier acuity, their higher frequency content can be used when separations are small, but as separation increases a smooth transition between the scales that determine threshold results in the continuum known as Weber's law for position. That is, with increasing separation, larger scales must be used, and thresholds increase in direct proportion to 1/frequency.

Keywords: Position; Vernier acuity; Weber's law

1. Introduction

The ability to accurately and veridically locate objects in visual space is essential for adaptive behaviour in our environment. Simple tasks, which we often take for granted, such as reaching and grasping, establishing positional relationships, obstacle avoidance and object tracking are vitally dependent upon this visual process. Real objects usually possess a variety of characteristics, each of which has the potential to affect our judgement of an objects' position. For example, we may choose to assign a unique visual location to an object based upon its entirety, either by judging the mid-point between its edges or by estimating the stimulus centroid (Hess & Holliday, 1996; Watt & Morgan, 1983; Watt, Morgan, & Ward, 1983; Whitaker, McGraw, Pacey, & Barrett, 1996). Alternatively, we may use the internal, local features within the boundaries of the object in order to establish its position relative to other features in the visual field (Barrett, Whitaker, & Bradley, 1999; Westheimer & McKee, 1977). In the present study we constrain observers to use different types of stimulus structure and examine how this affects the ability to localise objects relative to one another.

Perhaps the most compelling feature of human performance on relative localisation tasks is that positional accuracy usually varies in proportion to the separation of the objects concerned. This is known as 'Weber's law for position' and is consonant with physiological behaviour across a range of sensory modalities in which just-noticeable stimulus differences are proportional to the magnitude of the stimulus itself. The visual mechanisms which underlie Weber's law for position have been the subject of considerable investigation. The results of these studies point towards an important distinction between Weber's law behaviour based upon first-order luminance cues and second-order cues provided by the envelope of activity within the object as a whole (Akutsu, McGraw, & Levi, 1999; Burbeck, 1991; Burbeck & Yap, 1990; Levi & Westheimer, 1987). The former mechanism dominates at small separation levels, is optimal at high contrasts and iso-polarity, and exhibits

* Corresponding author. Fax: +44-1274-385570.
E-mail address: d.j.whitaker@bradford.ac.uk (D. Whitaker).

0042-6989/02/$ - see front matter
PII: S0042-6989(02)00030-5

strong spatial-frequency dependence (Levi & Westheimer, 1987; Whitaker, 1993; Whitaker & MacVeigh, 1991; Wilson, 1986). The latter behaviour is quite different in its lack of frequency, contrast and polarity dependence, and operates across large distances of visual space (Burbeck, 1987, 1988; Hess & Badcock, 1995; Kooi, De Valois, & Switkes, 1991; Levi & Klein, 1992; Levi & Waugh, 1996; Levi, Jiang, & Klein, 1990; Toet & Koenderink, 1988; Whitaker & Latham, 1997).

It is, as yet, unclear how these mechanisms relate to one another, and how they interact to result in the Weber's law behaviour found for typical broad-band stimuli containing a variety of stimulus characteristics. As Hess and Hayes (1994) point out, separating out the contributions of carrier modulation and stimulus envelope is not a simple matter. The present study examines this problem by using stimulus configurations in which component characteristics can be examined either in isolation or combination. The results demonstrate an elegant, seamless transition between thresholds based on different types of stimulus structure, one which represents an important characterisation of the human visual system.

2. Methods

2.1. Stimuli

Observers performed a two-element vernier alignment task in which the elements to be aligned were Gabor patches truncated along their inner horizontal midline (Fig. 1). These patches contain spatial structure in the form of the sinusoidal luminance modulation (carrier grating) within the patch, as well as structure in the form of the entire stimulus contrast envelope. Observers fixated between the two half-Gabor elements, but no explicit fixation point was provided.

Generation and control of stimuli was performed using the macro capabilities of the public domain software NIH Image™1.61 (developed at the U.S. National Institutes of Health and available from the Internet by anonymous FTP from zippy.nimh.nih.gov or on floppy disk from the National Technical Information Service, Springfield, Virginia, part number PB95-500195GEI). Stimuli were presented on a Mitsubishi 21" d2 colour display monitor with a mean luminance, L, of 38.3 cd m^{-2}, a frame rate of 75 Hz and an inter-pixel separation of 0.324 mm. The non-linear luminance response of the display was linearised by using the inverse function of the luminance response as measured with a Minolta CS-100 photometer. Contrast resolution of up to 12-bit accuracy was obtained by combining the red, green and blue outputs of the video board using a video summation device constructed according to Pelli and Zhang (1991). The host computer was a Motorola Starmax 4000/200 PowerPC.

The mathematical description of the stimuli is represented by the following equation:

$$L + \left[\exp \frac{-((x + (\alpha\delta x/2))^2 + (|y| - S/2)^2)}{2\sigma^2} \times \{LC(\sin(2\pi F(x + (\beta\delta x/2))))\} \right] \quad (1)$$

where x and y are the respective horizontal and vertical distances from the geometric centre of the element pair, F and C are the respective spatial frequency and contrast of the carrier grating, L is the mean luminance, σ is the standard deviation of the Gaussian envelope, S is the vertical edge-to-edge separation of the two elements and δx is the horizontal vernier offset between the envelopes and/or carriers of the two elements.

Three different stimulus implementations were investigated:

(1) Offsets were produced by horizontally displacing the envelope of the patches whose carrier remained fixed in vertical alignment. Thus, in Eq. 1,

$$\alpha = y/|y| \quad \text{and} \quad \beta = 0$$

Subjects were required to make a vernier judgement based upon the alignment of the envelope alone (Fig. 1a).

(2) Offsets were produced by horizontally displacing the carrier grating within the patches whose envelopes remained fixed in vertical alignment. With respect to Eq. 1,

$$\alpha = 0 \quad \text{and} \quad \beta = y/|y|$$

Subjects were required to make a vernier judgement based upon the alignment of the carrier grating alone (Fig. 1b).

(3) Carrier and envelope were yoked together in position and offsets were produced by an identical displacement of both of these stimulus characteristics. This is the stimulus condition typically used in studies of this kind. With respect to Eq. 1,

$$\alpha = y/|y| \quad \text{and} \quad \beta = y/|y|$$

Subjects could use either the carrier or envelope to base their vernier judgement (Fig. 1c).

The three types of stimuli were never interleaved within a run. Subjects always knew which type of stimulus was to be presented, and, hence, which type of judgement to make. It has previously been shown that observers can selectively attend either to the carrier or the envelope when making localisation judgements (Akutsu & Levi, 1998). Stimulus contrast, C, was maintained at a fixed suprathreshold level, 0.5 log units above the threshold for detection. Contrast thresholds were established using a method of adjustment with the cri-

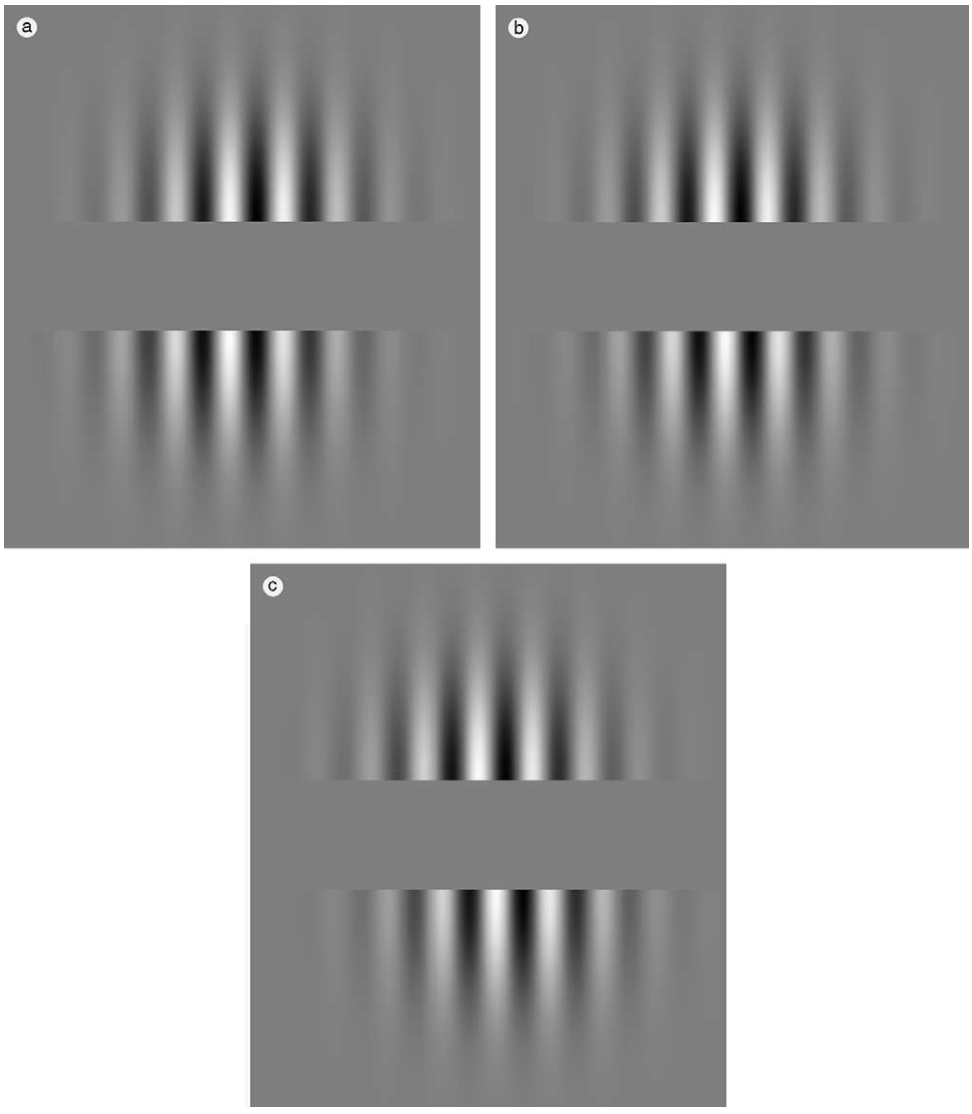

Fig. 1. (a) An example of the stimulus condition in which the carrier grating remains in alignment, but the envelope of the upper element is offset (in this case rightwards) relative to that in the lower element. (b) An example of the stimulus condition in which the contrast envelopes remain in alignment, but the carrier grating of the upper element is offset (in this case leftwards) relative to that in the lower element. (c) An example of the stimulus condition in which both the contrast envelope and the carrier grating of the upper element are offset (in this case leftwards) by an identical amount relative to those in the lower element.

terion of simultaneous detection of both vernier elements.

Two important stimulus parameters were examined in detail—these were the spatial frequency of the carrier grating and the separation between the two half-Gabors. Fig. 2 shows two examples of varying these parameters. In the examples chosen, the spatial frequency of the stimulus on the right is 32 times less than that on the left, whilst the gap is a factor of 32 times larger. Spatial frequencies of between 0.5 and 16 c deg^{-1} were examined. Gap sizes ranged from 0.125° to 64° of visual angle. For the majority of stimuli, the standard deviation of the Gaussian envelope, σ, was maintained at 0.66°. In a subsidiary experiment we also investigated σ values of 0.33° and 1.32°.

2.2. Subjects

Two of the authors acted as observers, having undertaken extensive practice sessions prior to data collection. Observers viewed the screen binocularly at viewing distances which varied between 3.5 m and 19.7 cm depending upon stimulus parameters. Data were collected under conditions of dim room illumination.

2.3. Procedure

On any trial the two half-Gabors were presented one above the other for a duration of 250 ms. Observers were then required to respond via the computer keyboard as to whether the relevant stimulus feature

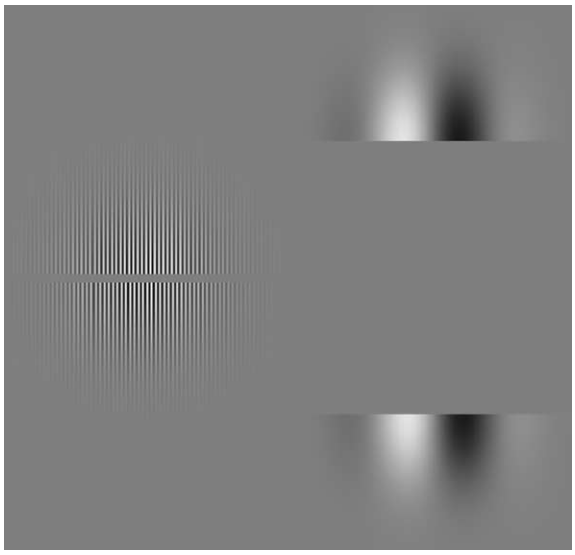

Fig. 2. Examples of two stimulus configurations, highlighting the two main variable stimulus characteristics examined in the present experiments. The left-hand stimulus contains a carrier grating of high spatial frequency, in which the upper and lower stimulus elements are separated by a small distance. The right-hand stimulus contains a carrier grating of low spatial frequency in which the upper and lower stimulus elements have a large separation.

(carrier, envelope or both) in the upper element was offset to the right or left of that in the lower element. No feedback was provided, thereby allowing the data to follow the subjects' internal alignment bias without contaminating threshold estimates. Care was taken to ensure that the stimulus elements were sufficiently distant from the horizontal edges of the CRT that positional judgements relative to the screen edge did not contribute to observer performance. Control experiments involving horizontal jitter of the stimulus elements confirmed this view. The use of jitter throughout the data collection was avoided so that the position of the stimulus elements could be maintained accurately above and below fixation. A second control experiment was used to exclude the possibility that local phase information contributed to performance. Careful scrutiny of Fig. 1a and b confirms the prediction that offset of the envelope relative to the carrier (or vice versa) produces local luminance cues within individual bars of the carrier grating which could potentially be used to interpret the direction of relevant feature offset. Whilst this would seem unlikely given the short exposure duration, the possibility was excluded from the results of control experiments in which the location of the irrelevant feature was randomised from trial to trial.

A method of constant stimuli was adopted, in which one of seven pre-determined feature offsets could be presented on any single trial. These offsets were chosen so that responses ranged from almost 100% leftward to almost 100% rightward. Twenty stimulus presentations were made at each of these stimulus offsets, producing 140 trials in total. The resulting responses were analysed by logistic regression to reveal the offset corresponding to the point of subjective equality (50% response point) and, more importantly, the alignment threshold (defined as half the distance between vernier offsets corresponding to 26.9 and 73.1% rightward responses).

3. Results

Fig. 3 shows vernier thresholds plotted against element separation for stimuli in which only the envelope of the stimuli was offset, the carrier remaining in alignment (Fig. 1a). Data for two observers are shown. Weber's law behaviour (proportionality between threshold and separation) is shown by the dashed line which corresponds to a Weber fraction of 0.7%. The different symbols represent data gathered at different carrier spatial frequencies. At all but very large separations,

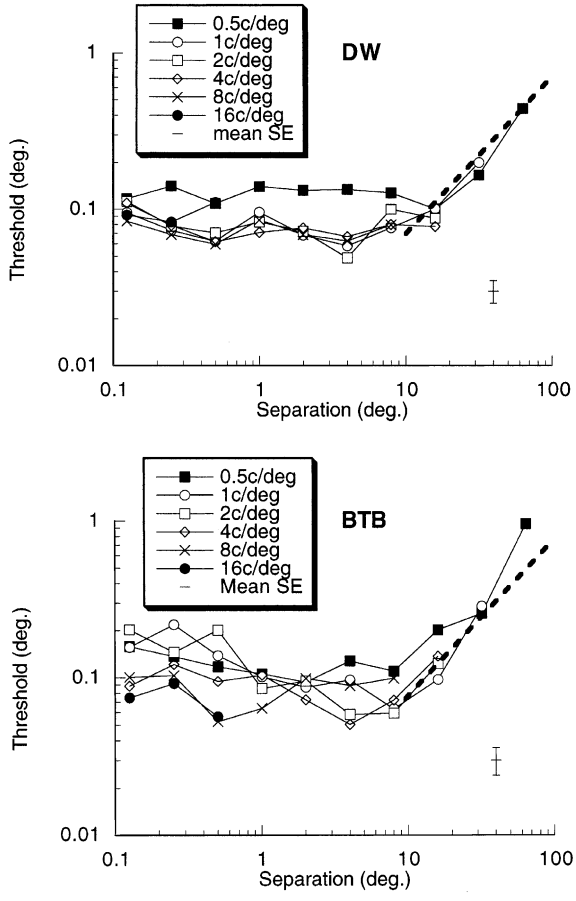

Fig. 3. Alignment thresholds plotted against element separation for the stimulus condition in which only the stimulus envelope was offset. At small separations, performance remains independent of separation at around 15% of the envelope size ($\sigma = 0.66°$) before rising in proportion to separation (Weber's law). The dashed lines represent Weber fractions corresponding to 0.7%. Different symbols represent different carrier frequencies as indicated in the legend.

thresholds appear independent of both separation and carrier spatial frequency (aside from a small spatial frequency effect for DW at the lowest frequency examined). Performance reaches a plateau at a threshold of approximately 0.1°, around 15% of the envelope σ (Toet, Eekhout, Simons, & Koenderink, 1987). Only when separation becomes very large does the trend appear to indicate an increase in thresholds in proportion to separation (Weber's law). Note that this behaviour is based upon data for the lowest spatial frequencies only, since higher frequencies were not sufficiently visible at these large separations/eccentricities.

These findings are consistent with previous data which suggest that the spread of the stimulus envelope enforces a lower limit on positional thresholds, rendering other stimulus characteristics ineffective (Burbeck, 1987; Toet & Koenderink, 1988). Since vernier thresholds for closely separated stimuli are inversely related to spatial frequency (Bradley & Skottun, 1987), and, since the envelope is a large Gaussian with energy primarily at low frequencies, the minimum thresholds in Fig. 3 never approach classic hyperacuity threshold levels. Evidence to confirm the importance of the envelope size, and hence its spatial frequency spectrum, is shown in Fig. 4.

Here we plot thresholds for detecting the offset of the stimulus envelope at a single carrier frequency (1 c deg^{-1}), but do so for three different values of envelope $\sigma - 0.33°$, 0.66° (taken from Fig. 3) and 1.32°. Data are fitted with a function of the form:

$$\text{Threshold} = \sqrt{\left(\frac{\text{Separation}}{k1}\right)^2 + (k2)^2} \qquad (2)$$

where $k1$ and $k2$ are constants. At small values of separation, thresholds are independent of separation and equal to $k2$. At large separations, thresholds begin to increase in proportion to separation, with a constant of proportionality $k1$. Again, data for very large separations is restricted by visibility. The plateau level at which thresholds remain independent of separation is clearly dependent upon the size of the envelope, representing approximately 10–16% of the envelope σ, in close agreement with the Gaussian blob alignment data of Toet et al. (1987). At very large separations, functions for each σ eventually converge to produce thresholds which increase according to Weber's law. Again, Weber fractions of just under 1% of patch separation are in close agreement with previous alignment data for both Gaussian blobs (Toet et al., 1987) and Gabor patches (Toet & Koenderink, 1988; Levi & Tripathy, 1996).

Fig. 5 shows data for the converse stimulus configuration—vernier offset of the carrier grating whilst the envelopes ($\sigma = 0.66°$) remain in alignment. Again, the different symbols represent data gathered at different carrier frequencies and the dashed line represents Weber's law behaviour. Data for different carrier frequencies no longer collapse together. Instead, higher frequency carriers result in lower vernier thresholds, at least at small separations (Bradley & Skottun, 1987). Individual functions for each carrier frequency remain fairly flat as separation increases before increasing beyond a certain critical separation. This critical separation increases with decreasing spatial frequency, indicating that higher spatial frequencies are more susceptible to the introduction of a gap between the stimulus elements (Whitaker, 1993; Whitaker & MacVeigh, 1991). The lower boundary of data across spatial frequencies corresponds reasonably well with Weber's law behaviour (dashed line, as in Figs. 3 and 4), at least for moderate and large values of separation. However, it is worth pointing out that this lower boundary is determined by successively higher spatial frequencies as separation is reduced.

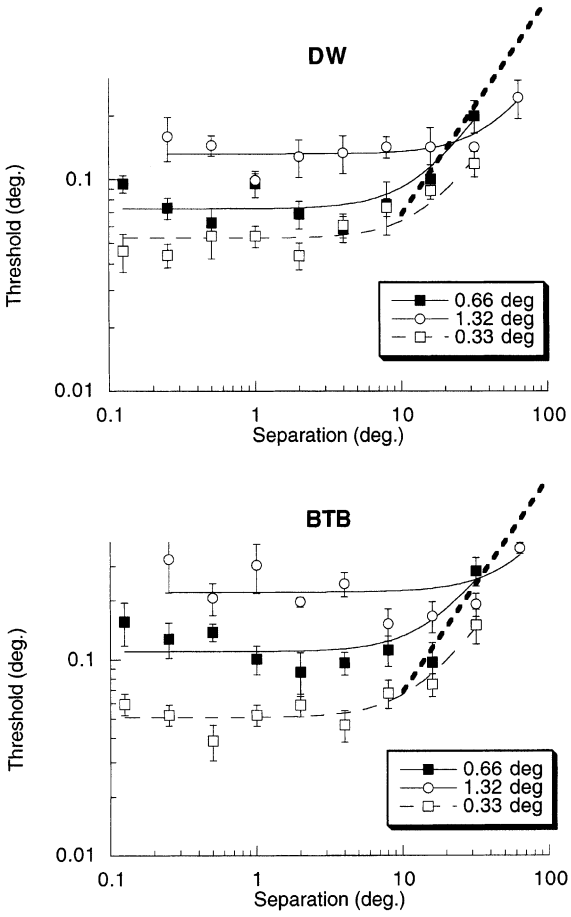

Fig. 4. Alignment thresholds for envelope judgements plotted against element separation for a single carrier frequency (1 c deg^{-1}), but three different envelope sizes whose σ is indicated in the legend. Curve fits represent best-fitting versions of Eq. 2 at each envelope size. Note how, for small and medium separations, performance is independent of separation yet depends strongly upon envelope size. At large separations, data from all envelope sizes converges to produce thresholds which increase as a function of separation (Weber's law). As in Fig. 3, dashed lines represent Weber fractions of 0.7%. Standard errors are shown.

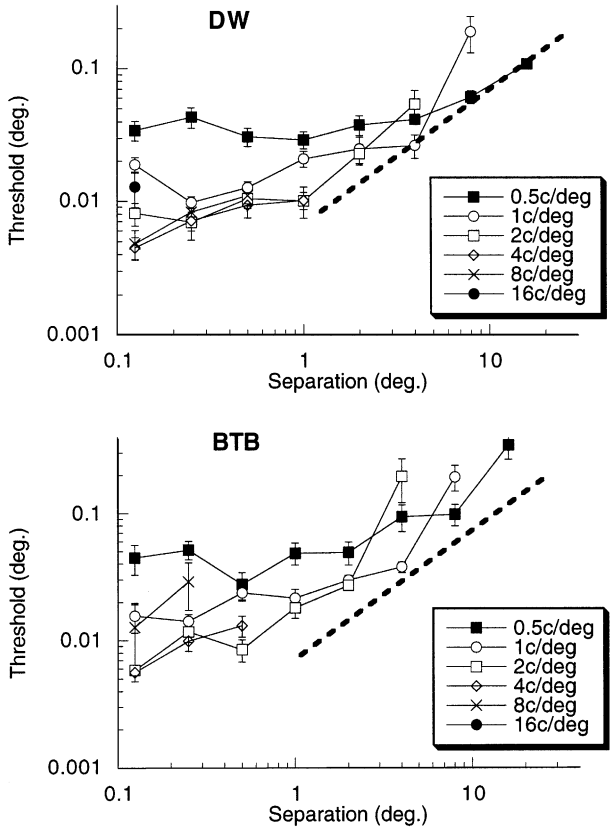

Fig. 5. Alignment thresholds for judging offset of the carrier grating, the envelopes always remaining in true alignment. Different symbols represent different carrier frequencies as indicated in the legend. Note how, at any separation, thresholds depend strongly upon carrier frequency. Functions for each frequency show a plateau at small separations before rising sharply above a certain separation (the right-most data point of each function represents the highest separation at which threshold measurements were possible). The envelope of lowest thresholds for each carrier frequency follow Weber's law (dashed line) fairly well. The lines represent Weber fractions of 0.7%. Standard errors are shown.

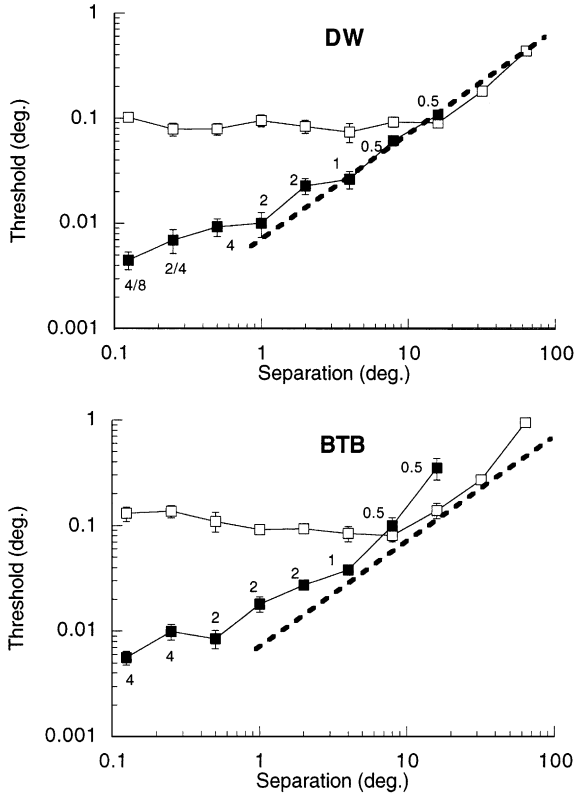

Fig. 6. Data from Figs. 3 and 5 replotted together. The open squares represent the mean alignment threshold, averaged across carrier frequency at each separation, for the envelope judgement task whose data are shown in Fig. 3. Filled squares represent optimum thresholds at each separation for the carrier judgement task whose data are shown in Fig. 5. Alongside these latter data points are numerals corresponding to the spatial frequency (in c deg^{-1}) which gave rise to the thresholds. For the open squares, error bars represent the standard error of the mean, whereas, for the filled squares, error bars represent the error of the individual threshold estimate. Note how both sets of data follow the same Weber relationship (dashed line), with carrier judgements dominating at small and medium separations before merging into the data for envelope judgments at large separations. Dashed lines represent Weber fractions of 0.7%.

Data from Figs. 3 and 5 are replotted together in Fig. 6. The mean envelope-offset thresholds (from Fig. 3), averaged across carrier frequency, are represented by open squares whilst the optimum carrier-offset thresholds (from Fig. 5) are represented by filled squares. Numerals alongside the carrier data represent the carrier spatial frequency which gave rise to these thresholds. The figure indicates that, at small to medium separations, thresholds mediated by judgement of carrier offset result in lower thresholds than those produced by judging the offset of the envelope. As separation is increased, the lower boundary of thresholds produced by the carrier judgements increases steadily in line with Weber's law, and is generated by successively lower carrier spatial frequencies. Since we cannot employ carrier frequencies with lower frequencies than the envelope, the carrier function eventually meets the envelope judgement data at moderately large values of separation. Beyond this level, the Weber's law behaviour is continued by the envelope data. In other words, judgements based upon carrier stimulus characteristics and, subsequently, envelope stimulus characteristics, dovetail neatly together to result in Weber's law behaviour over a large range of separations (approximately two orders of magnitude).

In the previous two experiments in which either the carrier or the envelope alone were offset, very different functions were obtained. We might therefore expect, if we present observers with the more typical situation in which the whole stimulus is offset (both carrier and envelope), that thresholds would follow the lower boundary set by the two different functions. We now describe the results from such an experiment. Fig. 7 shows data for this condition alongside data from the previous two conditions to allow inferences to be made as to whether

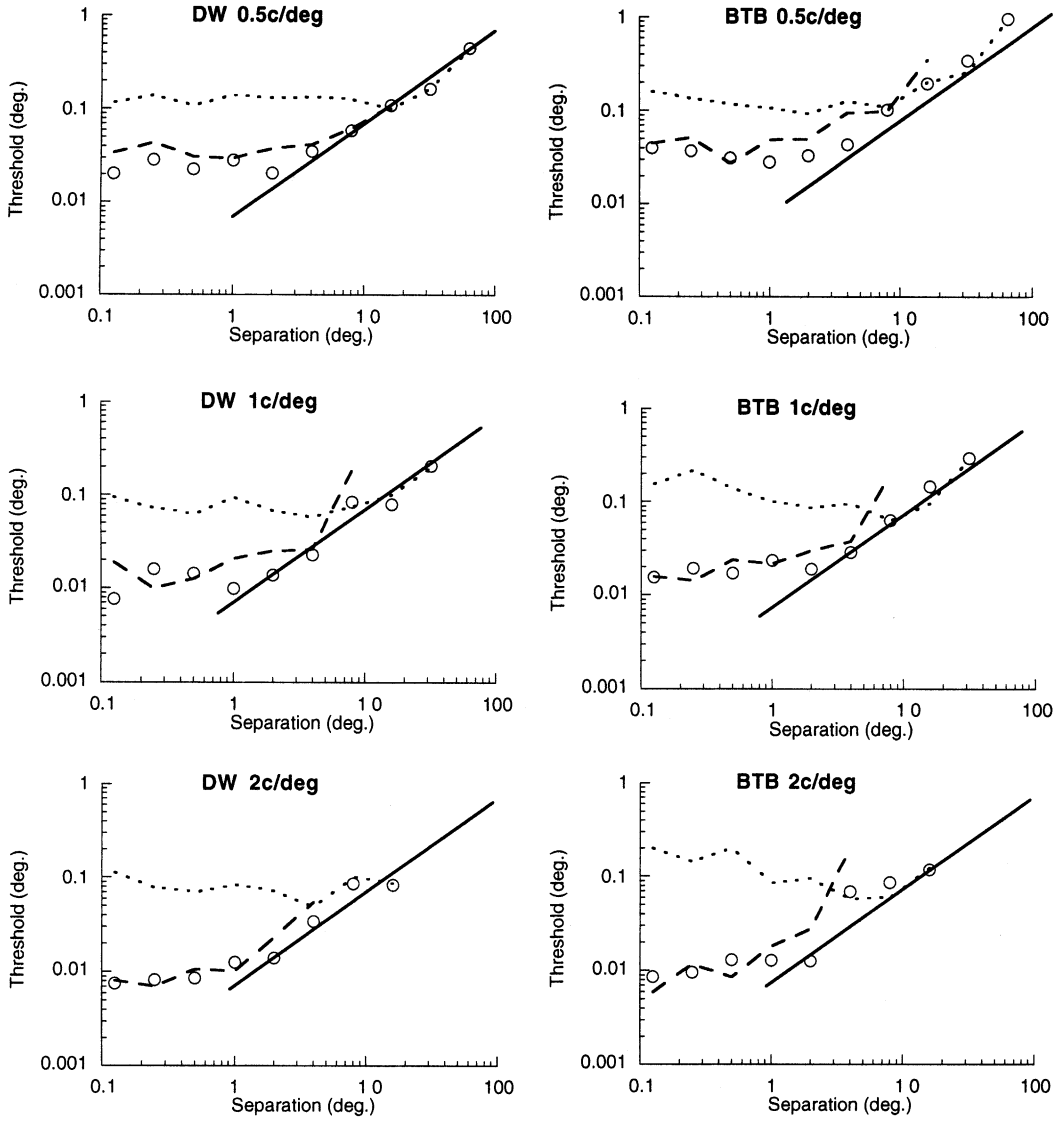

Fig. 7. Thresholds for judgement of envelope offset (dotted line, taken from Fig. 3), judgement of carrier offset (dashed line, taken from Fig. 5) and the condition in which both carrier and envelope were offset together (circles). Each plot shows a different carrier frequency (0.5–16 c deg^{-1}). At low and medium carrier frequencies, thresholds for the 'both' cue condition closely follow those for the 'carrier-only' condition when the separation is small. At larger separations the 'both' data break from the 'carrier-only' behaviour to follow the 'envelope-only' data thereafter. The abruptness of this transition is seen most clearly at moderate spatial frequencies (4–8 c deg^{-1}) and highlights the fact that observers are able to use either envelope or carrier cues to solve the typical type of vernier task in which both of these offset characteristics are present. The cue which observers use is critically dependent upon element separation. At the highest spatial frequency (16 c deg^{-1}), use of the carrier information becomes so difficult that thresholds for the 'both' condition simply follow the 'envelope-only' data. Indeed, a 'carrier-only' threshold could not be established for subject BTB at this very high spatial frequency. For all plots, solid lines represent a Weber fraction of 0.7%.

carrier envelope information is the determining factor for the combined condition thresholds. For low and medium carrier frequencies (0.5–2 c deg^{-1}), thresholds for the combined condition follow those for the carrier offset data (dashed line) almost exactly at low and medium separations before rising to join the envelope offset data (dotted line) at high values of separation. This trend is shown more clearly at higher carrier frequencies (4–8 c deg^{-1}) where there is a clear and sudden transition from threshold data which is determined by the carrier at small separations and envelope at large separations. At the very highest frequency (16 c deg^{-1}) observers consistently use the envelope at all separations.

4. Discussion

Physiological and psychophysical evidence for a linear, spatial-frequency tuned pathway which summates local luminance signals in primate vision was presented several decades ago (DeValois, Albrecht, & Thorell, 1982; Hubel & Wiesel, 1968). Whilst such mechanisms

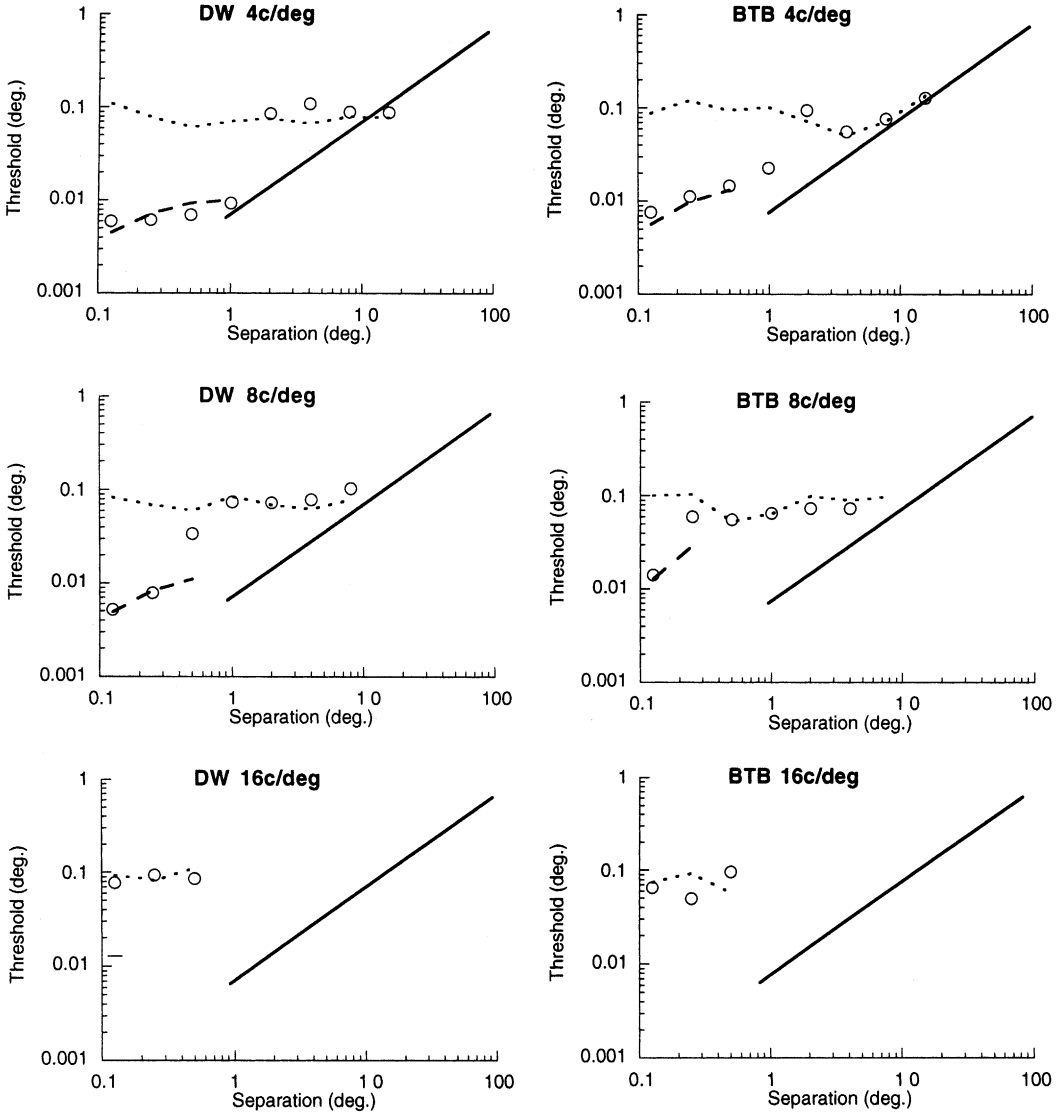

Fig. 7 (*continued*)

can be successfully applied to human performance in many tasks, including positional acuity (Wilson, 1986), certain stimulus configurations clearly require a form of analysis in which global stimulus structure is extracted in a non-linear fashion. In the context of the present experiments, positional judgements based upon the Gabor patch envelope require a non-linear processing stage to precede a subsequent stage of positional analysis. Physiological evidence for the existence of such a non-linear process is now available (Albright, 1992; Zhou & Baker, 1993). The combination of linear and non-linear processing of the Gabor patch results in the delivery of two neural signals to higher cortical levels. One of these takes the form of a narrow-band spike at the spatial frequency of the carrier, the other a relatively broad-band, low-pass spectrum corresponding to the Gaussian envelope of the stimulus, created by the early non-linearity. Either of these two signals could potentially be used by a mechanism responsible for positional analysis. As Bradley and Skottun (1987) have shown, alignment thresholds for closely spaced stimuli are directly proportional to spatial scale. In addition, the spatial extent (gap) over which alignment can be performed is also proportional to spatial scale, becoming impossible for gaps in excess of five spatial periods of the carrier grating (Whitaker, 1993). These considerations have clear implications for which of the two available neural signals might best be used for the various Gabor stimulus configurations used in the current study. At small separations, the higher-frequency, narrow-band signal resulting from the carrier would determine performance. Once a large enough gap is introduced, the broad band, low pass envelope signal must be used. This is exactly the transition we see in the data

of Fig. 7. A similar shift from high to low frequencies was observed using compound gratings by Barrett et al. (1999).

The picture which emerges is one of a shift to lower and lower spatial scales of first-order processing with increasing separation, eventually giving way to a dominance of second-order structure at separations which are sufficiently large to preclude the utility of information at scales finer than that of the stimulus envelope. A schematic explanation of this statement is shown in Fig. 8. When carrier information is available to contribute towards positional judgements, thresholds are determined by successively lower spatial scales as separation increases (Region A of Fig. 8). On an individual basis, such spatial scales do not, in themselves, demonstrate Weber's law behaviour, but the lower boundary of performance across a range of spatial scales mimics this effect. The reason why Weber's law is not evident with a single frequency stimulus (Whitaker, 1993; present study) is that there are no lower frequencies within the stimulus to shift to. Furthermore, repetitive stimuli, such as sinusoidal carrier gratings, begin to produce an ambiguous directional cue once the physical offset approaches half the period of the grating.

At separations beyond those which allow judgements based on the relevant carrier spatial frequency, performance assumes a level which is consistent with localisation thresholds based upon the envelope. The threshold vs separation function for this type of judgement demonstrates two important regions. In Region B (Fig. 8), thresholds are independent of separation, but demonstrate a dependence upon the size of the envelope. Localisation thresholds within this region therefore demonstrate no Weber's law behaviour. How might spatial scale considerations explain this type of behaviour? The absence of high spatial frequency information within the low-pass signal corresponding to the stimulus envelope will represent a limitation to any mechanism whose accuracy is proportional to spatial scale. Performance in this region will depend upon the size of the stimulus envelope (Fig. 4) since it is this which determines the scale of the highest frequencies within the low-pass envelope signal. Also, since the envelopes are quite large, the highest available envelope frequencies are very low, and such low frequencies can tolerate large separations before thresholds begin to rise (Fig. 5; Whitaker, 1993).

Once separation exceeds a critical level, the data obey Weber's law by demonstrating proportionality to separation (Region C). It is our assertion that performance in this region can also be explained on the basis of spatial scale. Although the highest spatial frequency in the non-linear representation of the envelope is low and can tolerate large separations, it too has a limit determined by its scale. Once this separation limit has been reached, lower frequencies in the envelope must be utilized with their corresponding higher thresholds. Thus, the multiple frequencies within the envelope signal produce Weber's law due to scale shifting that becomes necessary once separation is large enough. Predictably,

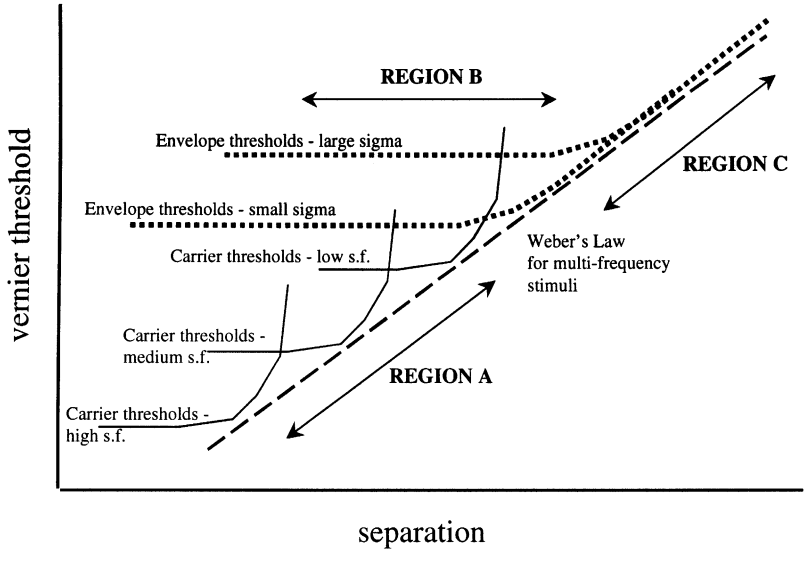

Fig. 8. A schematic to clarify the various factors which determine alignment thresholds across a range of element separations. At small separations, lowest vernier thresholds are produced by judgements based upon stimulus carrier offset. Successively lower carrier frequencies each possess self-similar threshold vs. separation functions which are displaced diagonally along both spatial axes (threshold and separation). The lower envelope of thresholds resulting from these functions represents Weber's law behaviour (Region A). At small separations, functions based upon envelope judgement demonstrate relatively poor vernier thresholds which are independent of separation but depend critically upon envelope size (Region B). At large separations these envelope functions individually demonstrate Weber's law behaviour (Region C). The Weber behaviour resulting from use of the carrier (Region A) and envelope (Region C) dovetail perfectly together to result in Weber's law behaviour across the entire separation range.

other more typical broad band stimuli (e.g. bars and lines) used for vernier tasks will have much lower thresholds than gaussian blobs or gabor envelopes and exhibit Weber's law due to scale shifting at much smaller separations (Waugh & Levi, 1995; Westheimer & McKee, 1977).

At least two potential explanations for the spatial scale shifts in Region C arise. The first is based upon the output of a non-linear filter of sufficiently large size to straddle the two stimulus elements. Such a process would offer an advantage in terms of parsimony since it essentially represents a similar type of process to that which is involved in analysing the carrier offset. These large filters would be responsive to the low-pass Gaussian signal of the stimulus envelope in much the same way as a large linear filter would be responsive to luminance-defined Gaussian blobs. Increasing separation would lead to Weber's law since it would determine the size of the smallest filter which straddled the two stimulus elements. Furthermore, in contrast to the carrier, the envelope signal is non-repetitive, meaning that there is no threshold restriction to the Weber's law behaviour. Nevertheless, since Weber's law extends to very large separations (at least 60 degrees—Fig. 3) the availability of fovea-centred filters of such huge size seems implausible. This, amongst other factors, led a number of researchers to consider an alternative explanation involving a two-filter approach in which the position of each element is established and subsequent analysis compares these position estimates (Klein & Levi, 1987; Morgan & Regan, 1987). Cortical magnification considerations would predict that the eccentricity of the stimulus elements constrains the scale of the smallest available filter, and hence the accuracy by which each element can be localised. A reduction in envelope size in this region cannot improve performance, since the finer scale mechanisms which this manipulation might have brought into play are simply not available at the relevant eccentricity. In other words eccentricity, rather than separation, is the determinant of Weber's law in Region C. Our particular stimuli were not designed to differentiate between these two possible explanations for Weber's law in Region C, since the stimuli were always positioned either side of fixation, meaning that separation and eccentricity co-varied. However, other studies have addressed this issue by positioning stimuli around an annulus centred upon fixation, thereby allowing separation to vary independently of eccentricity. This has been done for line and dot stimuli in addition to the type of second-order Gabor stimuli used in the present study (Burbeck & Yap, 1990; Levi & Klein, 1990; Levi & Tripathy, 1996; Levi, Klein, & Yap, 1988; Whitaker & Latham, 1997). The consistent finding of these studies is that, when stimulus separation is equal to or larger than eccentricity (as in the present study), it is the stimulus eccentricity, rather than separation, which represents the determining factor underlying Weber's law for position.

The novelty of the present study lies in the fact that, through careful choice of stimuli, we have been able to isolate the contribution of different stimulus characteristics to Weber's law for position. We are mindful to avoid the claim that the present findings represent previously undiscovered phenomena. Rather, they represent an amalgam of previous data which have proven difficult to reconcile. Each of the three important regions highlighted in Fig. 8 have previously received attention. Region A has been studied by Whitaker (1993) and Whitaker and MacVeigh (1991) using horizontally truncated sinusoidal gratings. The gratings were not windowed in the x-direction and, hence, second-order positional cues were irrelevant to the task. In agreement with the model depicted in Fig. 8, their results demonstrate a series of self-similar threshold vs separation functions separated along the diagonal according to spatial frequency. When plotted in period space, individual functions collapse together.

Positional judgements based upon second-order envelope cues (Regions B and C) have also been investigated. Hess and Hayes (1993) measured alignment thresholds for vertically separated Gabor patches. Offsets were produced by a shift of the entire patch, i.e. both carrier and envelope moved by the same amount. However, carrier offset cues are unlikely to have contributed to their measurements since the centre-to-centre separation of their patches always exceeded five cycles of the carrier rendering such cues largely unuseable (Whitaker, 1993). Hess and Hayes (1993) measured alignment thresholds in this region of moderate stimulus separation (their stimuli were separated by approximately 5–15 times the σ of the stimulus envelope) and found performance which was independent of separation. Our results based upon the alignment of stimulus envelope are in agreement with their findings, since this range represents separations of around 3–10° for our stimuli ($\sigma = 0.66°$—Fig. 6). Using stimuli of constant bandwidth (envelope size and carrier frequency scaled together), Hess and Hayes (1993) varied the carrier frequency of their stimuli and concluded that this was the factor which determined alignment threshold. Their interpretation was that neural recruitment of early, low-level spatial-frequency mechanisms was the key factor in determining changes in positional thresholds with increasing separation. However, since they co-varied carrier spatial frequency and envelope size an alternative interpretation—that the stimulus envelope determined performance—is also possible. That this is the most likely explanation of their findings is confirmed in our Fig. 4 where we demonstrate separation-independent regions in which the level of performance is determined by the size of the stimulus envelope for a fixed carrier spatial frequency. Hence, whilst we are in complete

agreement with Hess and Hayes (1993) that neural recruitment across low-level mechanisms of different spatial scales contributes towards Weber's law for position, we reach this conclusion for very different reasons. Our proposal (Fig. 8) is that a process of recruitment determines Weber's law in Region A of the figure through successive use of local, first-order spatial frequency content, whilst Weber's law in Region C is determined by recruitment across the broad-band, low-pass spectral characteristics of the stimulus envelope (Hess & Hayes, 1994). It is relevant, and confirmatory to our argument, to note that studies which have investigated the localisation of first-order, luminance-defined Gaussian blobs, find the same pattern of behaviour as we find in Regions B and C—a performance plateau at small separations rising to Weber's law at large separations (Toet et al., 1987; Williams, Enoch, & Essock, 1984). In addition, as several authors have shown (Burbeck, 1987, 1988; Kooi et al., 1991; Levi & Tripathy, 1996; Toet & Koenderink, 1988), thresholds in the ascending region of the function (Region C) are largely immune to variations in the spatial frequency content of the stimuli. Thus, whether the Gaussian signal is explicit, in the form of a luminance modulation, or implicit, in the form of a second-order contrast modulation, identical effects are found.

Several other findings are entirely consistent with a model in which different scales of carrier or envelope parameters can determine visual performance depending upon stimulus characteristics. Akutsu et al. (1999) investigated the alignment of Gabor patches with asymmetric contrast envelopes. When the patches were separated by a distance which was a large multiple of the carrier period, alignment was consistent with the use of the centroid of the contrast envelope (Whitaker et al., 1996). At smaller separations the data converged towards that expected based upon alignment of the carrier. Barrett et al. (1999) measured alignment thresholds for compound carrier gratings consisting of a fundamental and its third harmonic. When the gratings were abutting, thresholds were consistent with the use of the higher frequency third harmonic. However, the introduction of a gap between the gratings led to a domination of performance by the fundamental, i.e. a shift to lower carrier spatial frequencies occurred as a function of separation.

There is, however, evidence to suggest that spatial scale considerations alone are insufficient to account for Weber's law for position. This comes from masking studies in which positional relationships between broad-band dot and line targets are examined in the presence of relatively narrow-band noise masks (Levi & Waugh, 1996; Waugh & Levi, 1995; Waugh, Levi, & Carney, 1993). Whilst the peak masking effect does reduce in spatial frequency as a function of separation, it does so only at relatively large values of separation (Waugh & Levi, 1995). Thus, although alignment thresholds are already on the increase for separation values beyond 6′ of arc, the peak masking effect remains constant at around 10 c deg^{-1} up to a separation of approximately 30' arc before shifting to lower frequencies. Other sources of noise such as positional uncertainty in peripheral vision have therefore been suggested as imposing a limit upon performance (Waugh & Levi, 1993, 1995; Wilson, 1991).

How can findings of constancy of peak masking effect be reconciled with direct evidence of a shift in spatial scale with increasing separation? For small gap sizes, the use of mechanisms tuned to frequencies higher than 10 c deg^{-1} is likely to be limited by their reduced contrast sensitivity. As gap size increases, mechanisms tuned to lower frequencies are more likely to resist the gap, yet, due to their increased size, cannot produce such low alignment thresholds. In this way, a range of spatial mechanisms may produce approximately similar levels of performance, and this may be the reason why masking functions become much broader as gap size increases (Waugh & Levi, 1995). Relatively high frequency mechanisms (such as that at 10 c deg^{-1}) may still determine performance up to a gap of several times their spatial period (evidence for this type of effect is shown in Figs. 5 and 6). This may contribute to the observation that peak masking effects are shifted to larger gap sizes than suggested by alignment thresholds. Furthermore, it may be revealing to investigate peak masking functions using masks of constant visibility, rather than constant contrast as used in previous masking studies (Levi & Waugh, 1996; Waugh & Levi, 1995). It is predictable that masks of constant contrast will fail to demonstrate significant masking effects at very low or very high spatial frequencies due to poor contrast sensitivity, thus potentially underestimating the spatial frequency range over which masking effects occur.

The present findings suggest that consideration of spatial scale effects is critical for understanding positional relationships of first- and second-order stimuli. For the types of stimuli used in the present study, an early non-linearity would make available two signals of differing spatial scale. One signal would be at the scale of the carrier, with its magnitude related to the contrast of the carrier grating. The other signal would be at the scale of the envelope, with a magnitude related to the extent of the early non-linearity. Observers are able to select either of these signals to make a positional judgement, with stimulus configuration being the factor which determines their relative importance. Thus, at small separations, the higher spatial frequency of the carrier is of most use, whilst at large separations the visual system has to resort to the lower spatial frequency, non-periodic envelope signal. These considerations avoid the need to invoke a specialised second-order position mechanism.

In summary, through careful choice of stimuli, we have been able to provide an insight into the individual contributions of first- and second-order mechanisms towards Weber's law for position. The picture which emerges is one of a spatial-scale dependent contribution from the various stimulus characteristics which are typically contained within objects in the visual world.

Acknowledgements

PVM is a Wellcome Trust Research Development Fellow. The authors wish to acknowledge the helpful comments of the reviewers on an earlier draft of this manuscript.

References

Akutsu, H., & Levi, D. M. (1998). Selective attention to specific location cues: the peak and center of a patch are equally accessible as location cues. *Perception, 27*, 1015–1023.

Akutsu, H., McGraw, P. V., & Levi, D. M. (1999). Alignment of separated patches: multiple location tags. *Vision Research, 39*, 789–801.

Albright, T. (1992). Form-cue invariant motion processing in primate visual cortex. *Science, 255*, 1141–1143.

Barrett, B. T., Whitaker, D., & Bradley, A. (1999). Vernier acuity with compound gratings: the whole is equal to the better of its parts. *Vision Research, 39*, 3681–3691.

Bradley, A., & Skottun, B. C. (1987). Effects of contrast and spatial frequency on vernier acuity. *Vision Research, 27*, 1817–1824.

Burbeck, C. A. (1987). Position and spatial-frequency in large-scale localization judgements. *Vision Research, 27*, 417–427.

Burbeck, C. A. (1988). Large-scale relative localization across spatial frequency channels. *Vision Research, 28*, 857–859.

Burbeck, C. A. (1991). Encoding spatial relations. In R. J. Watt (Ed.), *Pattern recognition by man and machine* (pp. 8–18). London: Macmillan Press.

Burbeck, C. A., & Yap, Y. L. (1990). Two mechanisms for localization? Evidence for separation-dependent and separation-independent processing of position information. *Vision Research, 30*, 739–750.

DeValois, R. L., Albrecht, D. G., & Thorell, L. G. (1982). Spatial frequency selectivity of cells in macaque visual cortex. *Vision Research, 22*, 545–559.

Hess, R. F., & Badcock, D. R. (1995). Metric for separation discrimination by the human visual system. *Journal of the Optical Society of America A, 12*, 3–16.

Hess, R. F., & Hayes, A. (1993). Neural recruitment explains "Weber's law" of spatial position. *Vision Research, 33*, 1673–1684.

Hess, R. F., & Hayes, A. (1994). The coding of spatial position by the human visual system—effects of spatial scale and retinal eccentricity. *Vision Research, 34*, 625–643.

Hess, R. F., & Holliday, I. E. (1996). Primitives used in the spatial localization of nonabutting stimuli: peaks or centroids? *Vision Research, 36*, 3821–3826.

Hubel, D. H., & Wiesel, T. N. (1968). Receptive fields and functional architecture of monkey striate cortex. *Journal of Physiology, 195*, 215–243.

Klein, S. A., & Levi, D. M. (1987). Position sense of the peripheral retina. *Journal of the Optical Society of America A, 4*, 3–16.

Kooi, F. L., De Valois, R. L., & Switkes, E. (1991). Spatial localization across channels. *Vision Research, 31*, 1627–1631.

Levi, D. M., & Klein, S. A. (1990). The role of separation and eccentricity in encoding position. *Vision Research, 30*, 557–585.

Levi, D. M., & Klein, S. A. (1992). "Weber's law" for position: the role of spatial frequency and contrast. *Vision Research, 32*, 2235–2250.

Levi, D. M., & Tripathy, S. P. (1996). Localization of a peripheral patch: the role of blur and spatial frequency. *Vision Research, 36*, 3785–3803.

Levi, D. M., & Waugh, S. J. (1996). Position acuity with opposite polarity features: evidence for a non-linear collator mechanism for position acuity? *Vision Research, 36*, 573–588.

Levi, D. M., & Westheimer, G. (1987). Spatial-interval discrimination in the human fovea: what delimits the interval? *Journal of the Optical Society of America A, 4*, 1304–1313.

Levi, D. M., Jiang, B., & Klein, S. A. (1990). Spatial interval discrimination with blurred lines: black and white are separate but not equal at multiple spatial scales. *Vision Research, 30*, 1735–1750.

Levi, D. M., Klein, S. A., & Yap, Y. L. (1988). "Weber's Law" for position: Unconfounding the role of separation and eccentricity. *Vision Research, 28*, 597–603.

Morgan, M. J., & Regan, D. (1987). Opponent model for line interval discrimination: interval and vernier performance compared. *Vision Research, 27*, 107–118.

Pelli, D. G., & Zhang, L. (1991). Accurate control of contrast on microcomputer displays. *Vision Research, 31*, 1337–1350.

Toet, A., & Koenderink, J. J. (1988). Differential spatial discrimination thresholds for Gabor patches. *Vision Research, 28*, 133–143.

Toet, A., Eekhout, M. P., Simons, H. L. J., & Koenderink, J. J. (1987). Van Scale invariant features of differential spatial displacement discrimination. *Vision Research, 27*, 441–451.

Watt, R. J., & Morgan, M. J. (1983). The recognition and representation of edge blur: evidence for spatial primitives in human vision. *Vision Research, 23*, 97–109.

Watt, R. J., Morgan, M. J., & Ward, R. M. (1983). Stimulus features that determine the visual location of a bright bar. *Investigative Ophthalmology and Visual Science, 24*, 66–71.

Waugh, S. J., & Levi, D. M. (1993). Visibility, luminance and vernier acuity. *Vision Research, 33*, 527–538.

Waugh, S. J., & Levi, D. M. (1995). Spatial alignment across gaps: contributions of orientation and spatial scale. *Journal of the Optical Society of America A, 12*, 2305–2317.

Waugh, S. J., Levi, D. M., & Carney, T. (1993). Orientation, masking and vernier acuity for line targets. *Vision Research, 12*, 1619–1638.

Westheimer, G., & McKee, S. P. (1977). Spatial configurations for hyperacuity. *Vision Research, 17*, 941–947.

Whitaker, D. (1993). What part of a vernier stimulus determines performance? *Vision Research, 33*, 27–32.

Whitaker, D., & Latham, K. (1997). Disentangling the role of spatial scale, separation and eccentricity in Weber's law for position. *Vision Research, 37*, 515–524.

Whitaker, D., & MacVeigh, D. (1991). Interaction of spatial frequency and separation in vernier acuity. *Vision Research, 31*, 1205–1212.

Whitaker, D., McGraw, P. V., Pacey, I., & Barrett, B. T. (1996). Centroid analysis predicts visual localization of first- and second-order stimuli. *Vision Research, 36*, 2957–2970.

Williams, R. A., Enoch, J. M., & Essock, E. A. (1984). The resistance of selected hyperacuity configurations to retinal image degradation. *Investigative Ophthalmology and Visual Science, 25*, 389–399.

Wilson, H. R. (1986). Responses of spatial mechanisms can explain vernier acuity. *Vision Research, 26*, 453–469.

Wilson, H. R. (1991). Model of peripheral and amblyopic hyperacuity. *Vision Research, 31*, 967–982.

Zhou, Y.-X., & Baker, C. L. (1993). A processing stream in mammalian visual cortex neurons for non-Fourier responses. *Science, 261*, 98–101.